RSC Advances (Electronic Supplementary Information)

# Role of cation choice in the radiation tolerance of pyrochlores

**Ram Devanathan,*[a] Fei Gao[a] and Christina J. Sundgren[a]**
[a]Chemical & Materials Sciences Division, MS K2-01
Pacific Northwest National Laboratory, Richland, WA 99352 USA.
Fax: 509-371-6242; Tel: 509-371-6487; E-mail: ram.devanathan@pnnl.gov

Table I. Number of Gd bond defects for radial distance (in the X-Y plane) less than 2 nm, between 2 and 2.8 nm, and beyond 2.8 nm from the center of the thermal spike.

| Composition | r < 2 nm | 2 nm < r < 2.8 nm | r > 2.8 nm |
|---|---|---|---|
| $Gd_2Zr_2O_7$ | 1580 | 1273 | 181 |
| $Gd_2Ti_{0.5}Zr_{1.5}O_7$ | 1587 | 1048 | 117 |
| $Gd_2TiZrO_7$ | 1574 | 789 | 53 |
| $Gd_2Ti_{1.5}Zr_{0.5}O_7$ | 1657 | 518 | 21 |
| $Gd_2Ti_2O_7$ | 1710 | 234 | 1 |

Table II. Number of B site (Zr or Ti) bond defects for radial distance (in the X-Y plane) less than 2 nm, between 2 and 2.8 nm, and beyond 2.8 nm from the center of the thermal spike.

| Composition | r < 2 nm | 2 nm < r < 2.8 nm | r > 2.8 nm |
|---|---|---|---|
| $Gd_2Zr_2O_7$ | 1501 | 1188 | 173 |
| $Gd_2Ti_{0.5}Zr_{1.5}O_7$ | 1351 | 912 | 125 |
| $Gd_2TiZrO_7$ | 1242 | 645 | 27 |
| $Gd_2Ti_{1.5}Zr_{0.5}O_7$ | 913 | 425 | 18 |
| $Gd_2Ti_2O_7$ | 903 | 179 | 20 |

Table III. Number of O bond defects for radial distance (in the X-Y plane) less than 2 nm, between 2 and 2.8 nm, and beyond 2.8 nm from the center of the thermal spike.

| Composition | r < 2 nm | 2 nm < r < 2.8 nm | r > 2.8 nm |
|---|---|---|---|
| $Gd_2Zr_2O_7$ | 644 | 381 | 86 |
| $Gd_2Ti_{0.5}Zr_{1.5}O_7$ | 978 | 513 | 65 |
| $Gd_2TiZrO_7$ | 1515 | 501 | 53 |
| $Gd_2Ti_{1.5}Zr_{0.5}O_7$ | 2446 | 461 | 18 |
| $Gd_2Ti_2O_7$ | 2723 | 254 | 2 |

Electronic Supplementary Material (ESI) for RSC Advances


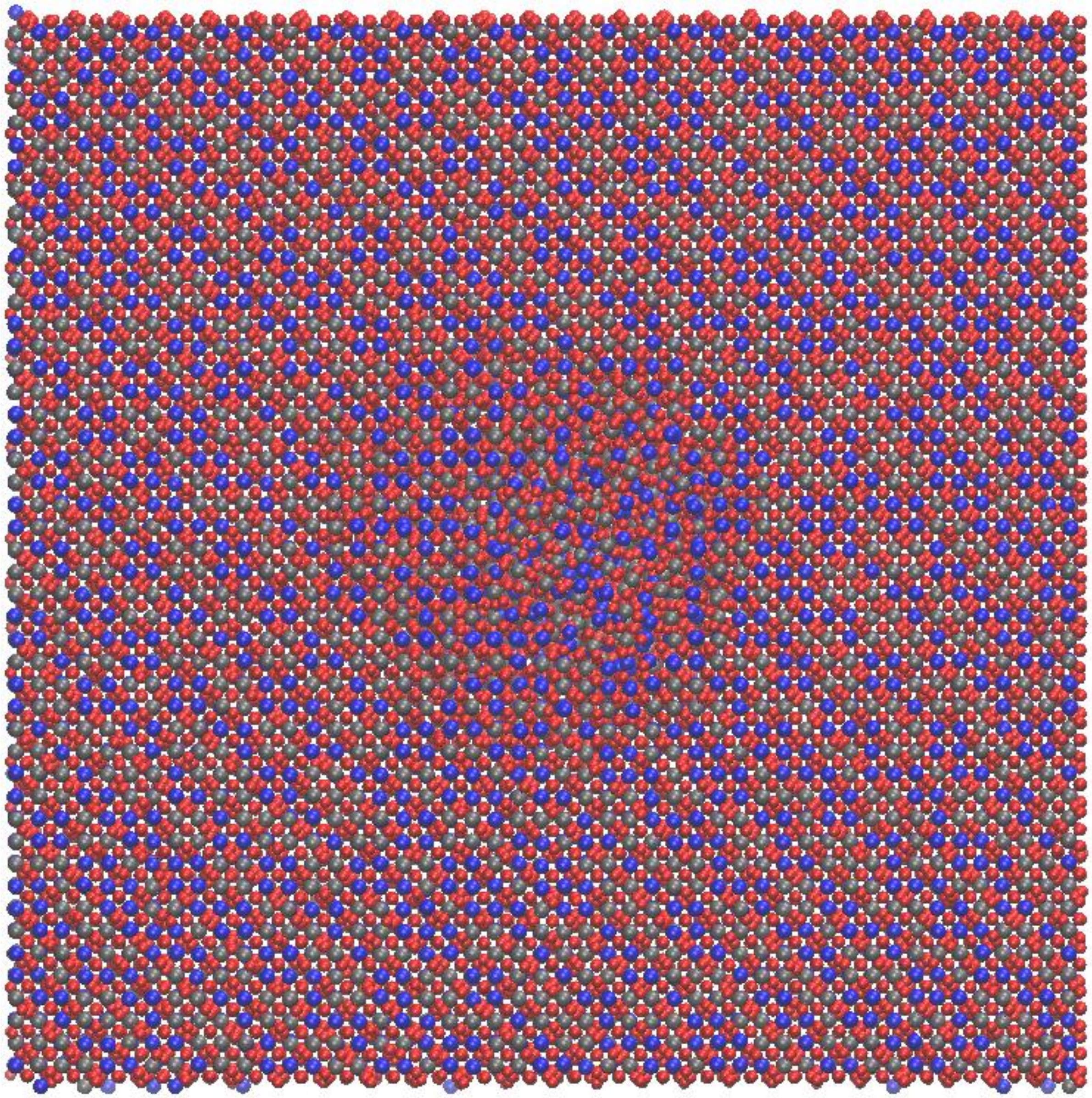

**Fig. S1** Projection of atom positions in $Gd_2Ti_{1.5}Zr_{0.5}O_7$ at ~50 ps after a 12 keV/nm thermal spike. The side length is ~12.5 nm. Gd is shown as a blue sphere, Zr and Ti as grey spheres, and O as a red sphere.

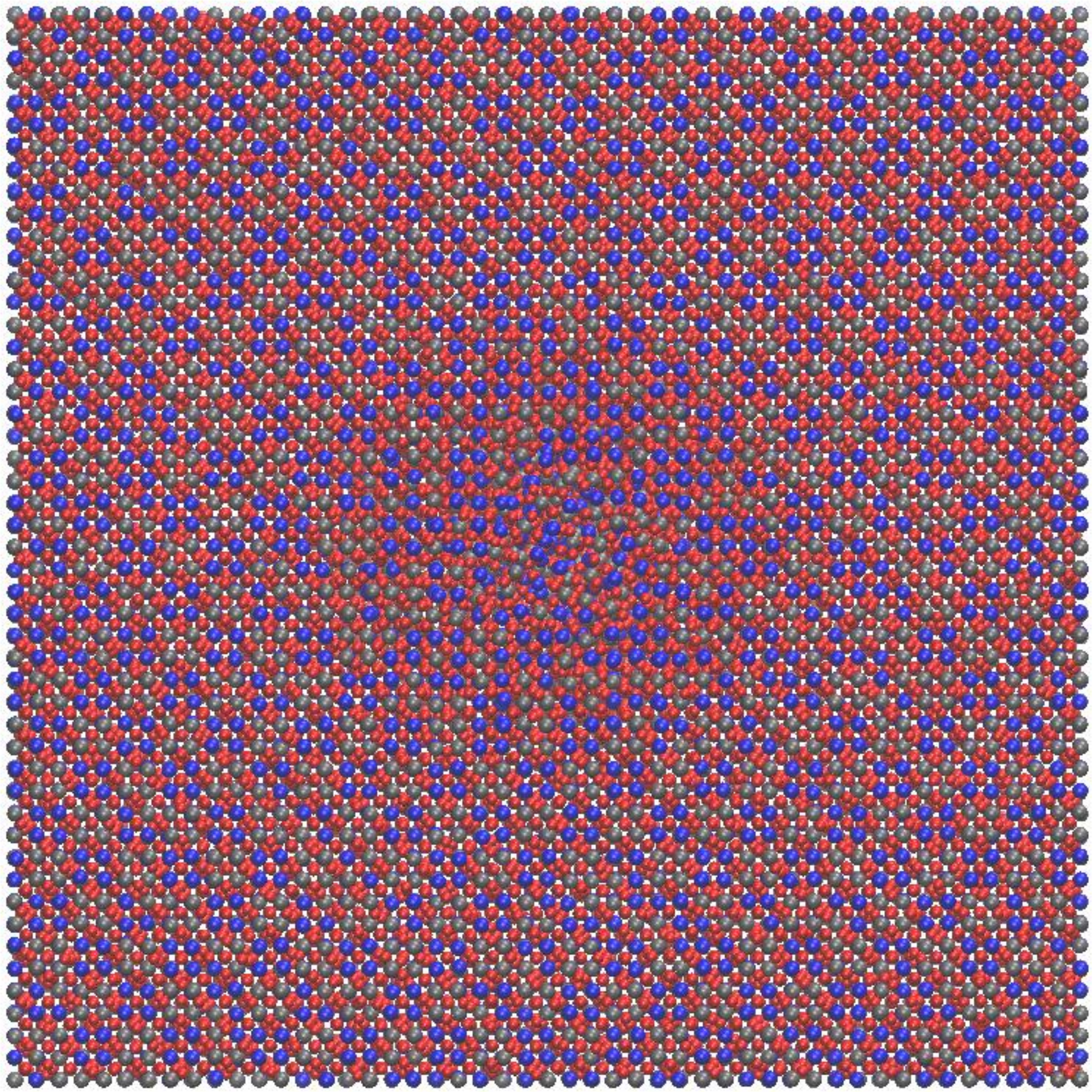

**Fig. S2** Projection of atom positions in $Gd_2TiZrO_7$ at ~50 ps after a 12 keV/nm thermal spike. The side length is ~12.5 nm. Gd is shown as a blue sphere, Zr and Ti as grey spheres, and O as a red sphere.

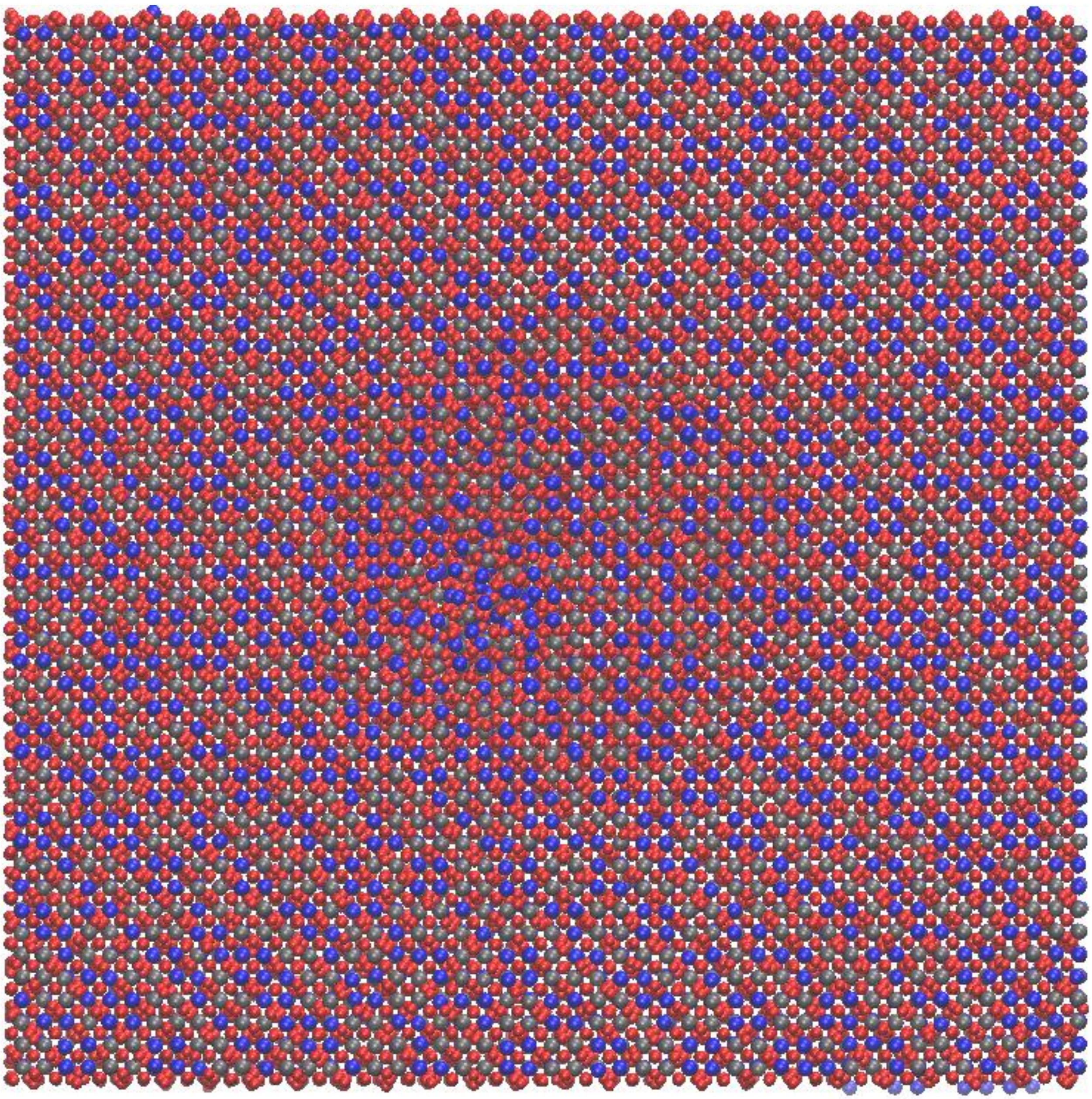

**Fig. S3** Projection of atom positions in $Gd_2Ti_{0.5}Zr_{1.5}O_7$ at ~50 ps after a 12 keV/nm thermal spike. The side length is ~12.5 nm. Gd is shown as a blue sphere, Zr and Ti as grey spheres, and O as a red sphere.

Electronic Supplementary Material (ESI) for RSC Advances


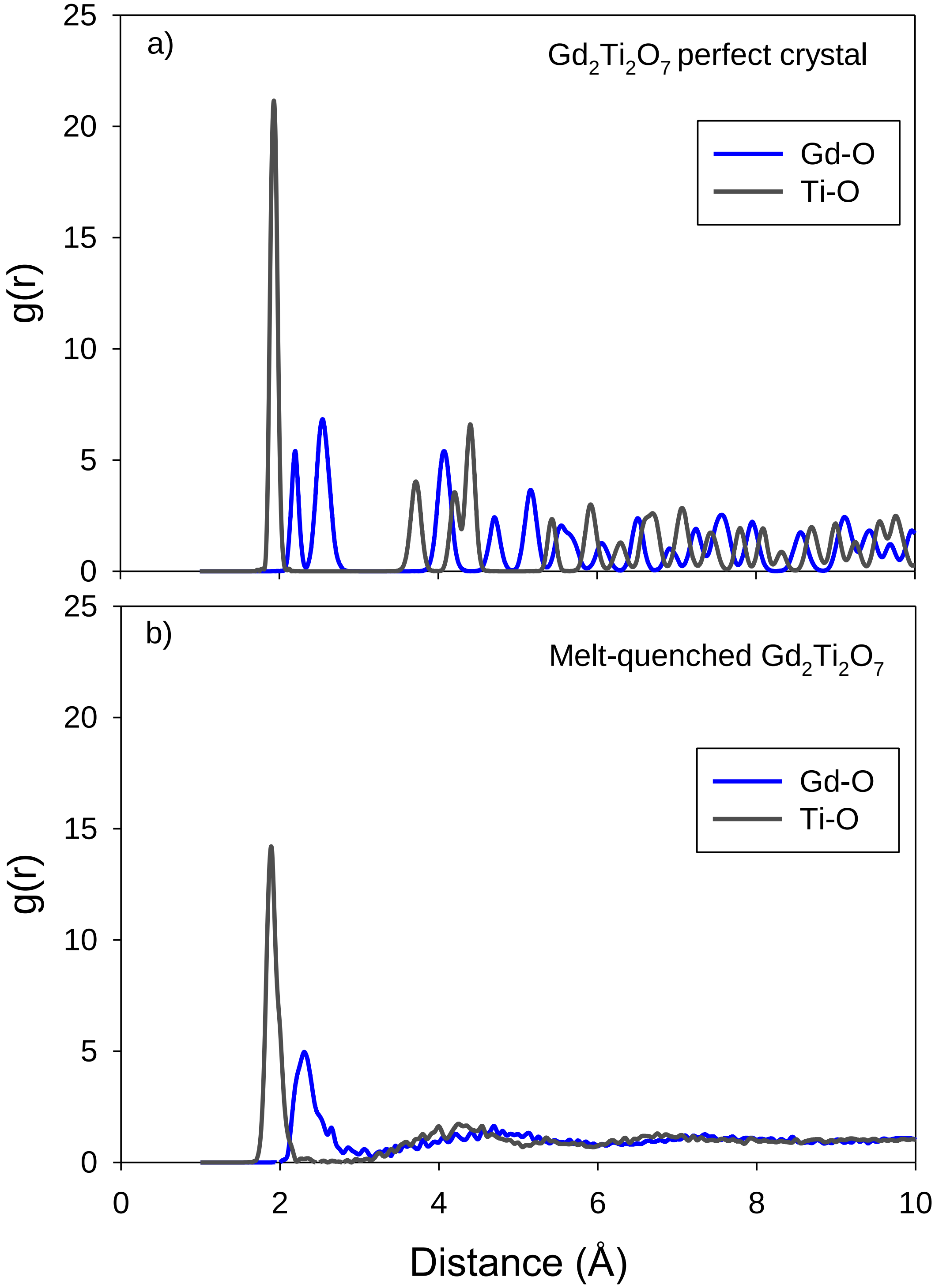


;

**Fig. S4** Radial distribution functions of Gd-O and Ti-O pairs in a) perfectly crystalline and b) melt-quenched amorphous $Gd_2Ti_2O_7$ at 300 K.

Electronic Supplementary Material (ESI) for RSC Advances
This journal is © The Royal Society of Chemistry 2013

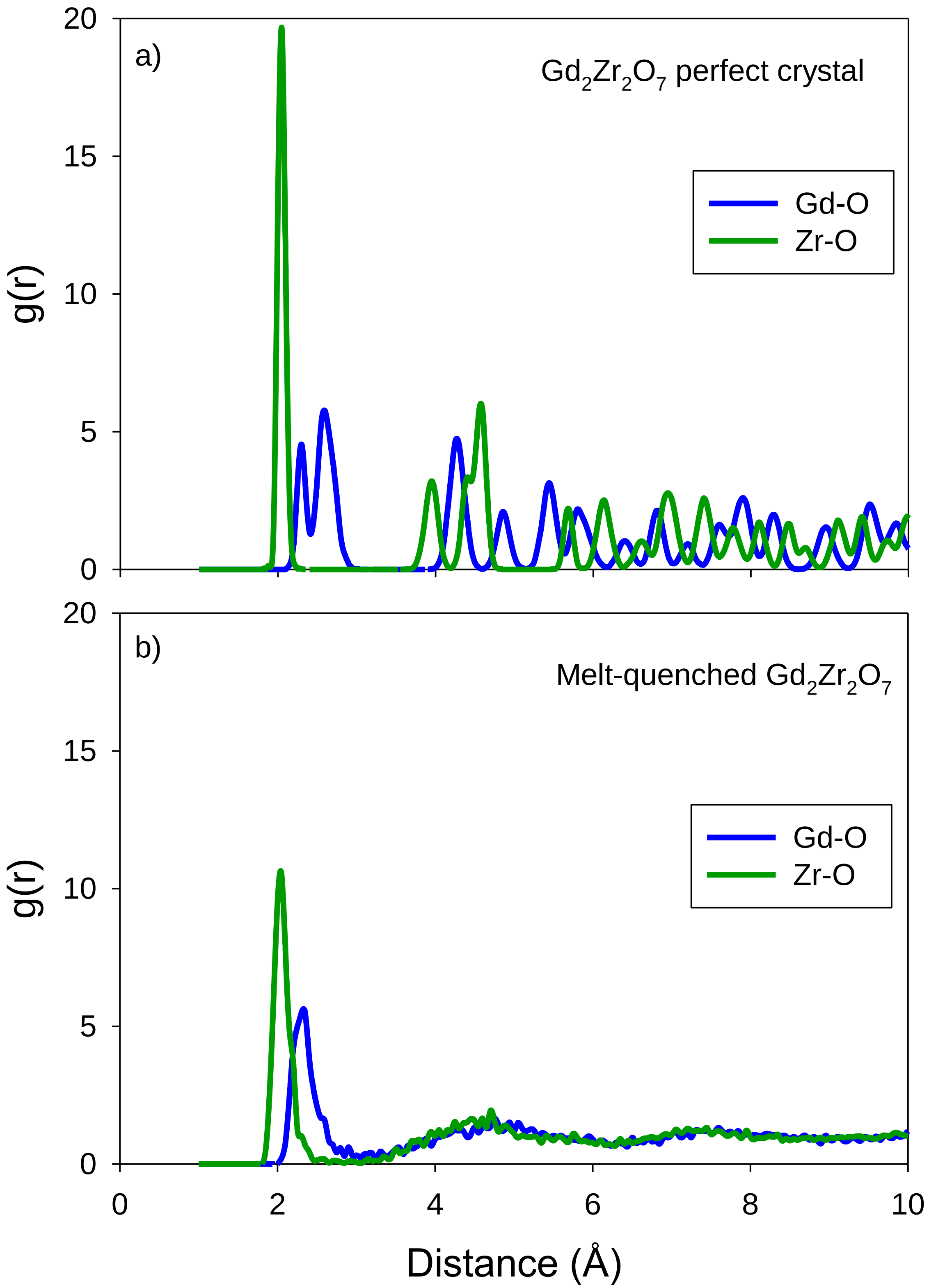


**Fig. S5** Radial distribution functions of Gd-O and Zr-O pairs in a) perfectly crystalline and b) melt-quenched amorphous $Gd_2Zr_2O_7$ at 300 K.

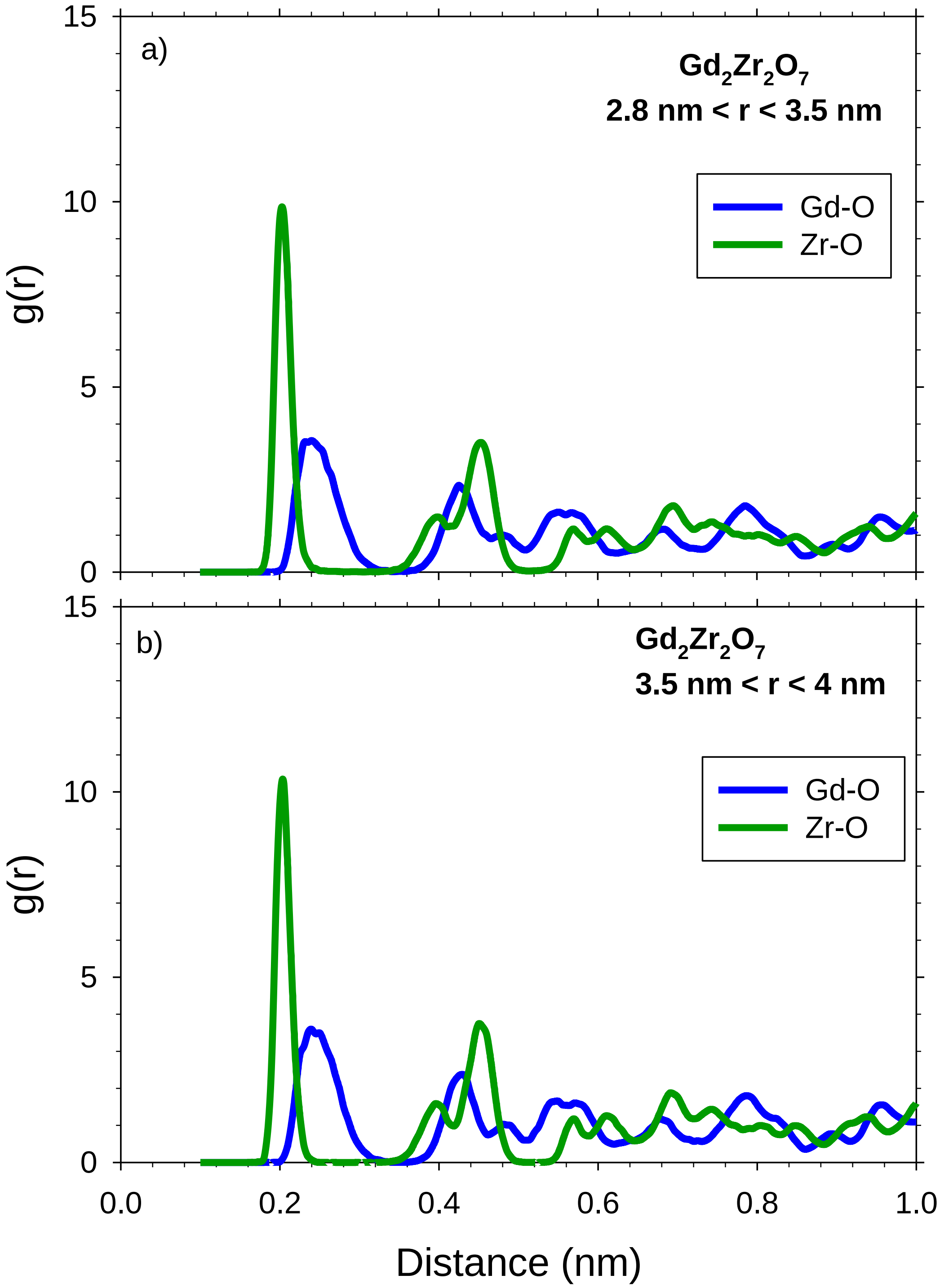


**Fig. S6** Radial distribution functions of Gd-O and Zr-O pairs in annular cylinders centered on a 12 keV/nm thermal spike with a) radius between 2.8 and 3.5 nm; and b) radius between 3.5 and 4 nm in $Gd_2Zr_2O_7$.

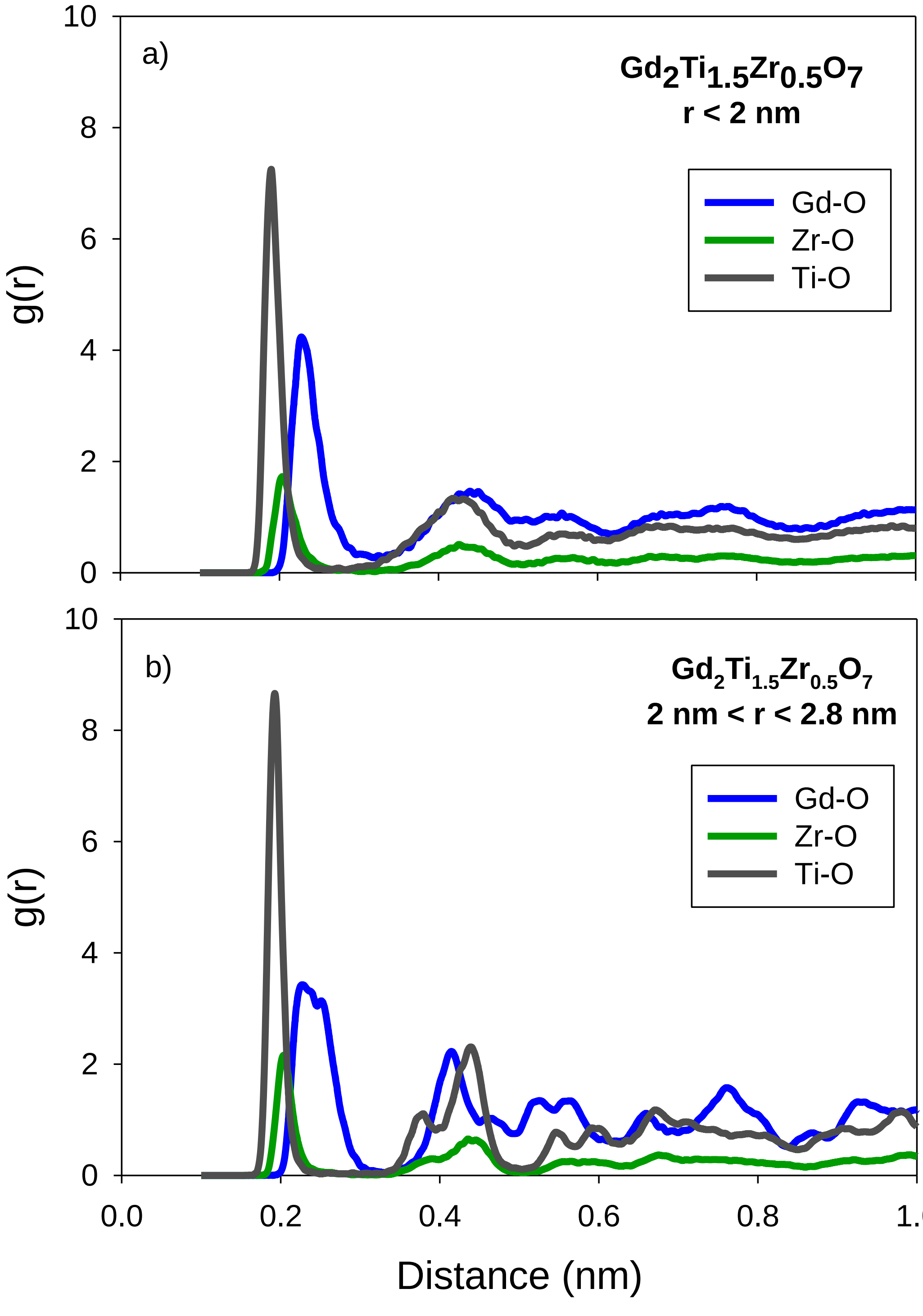


**Fig. S7** Radial distribution functions of Gd-O, Zr-O, and Ti-O pairs in a) the damage core and b) damage periphery in $Gd_2Ti_{1.5}Zr_{0.5}O_7$ subjected to a thermal spike with energy deposition of 12 keV/nm at 300 K. The core is amorphous while the periphery shows broad peaks characteristic of disordered pyrochlore crystal.

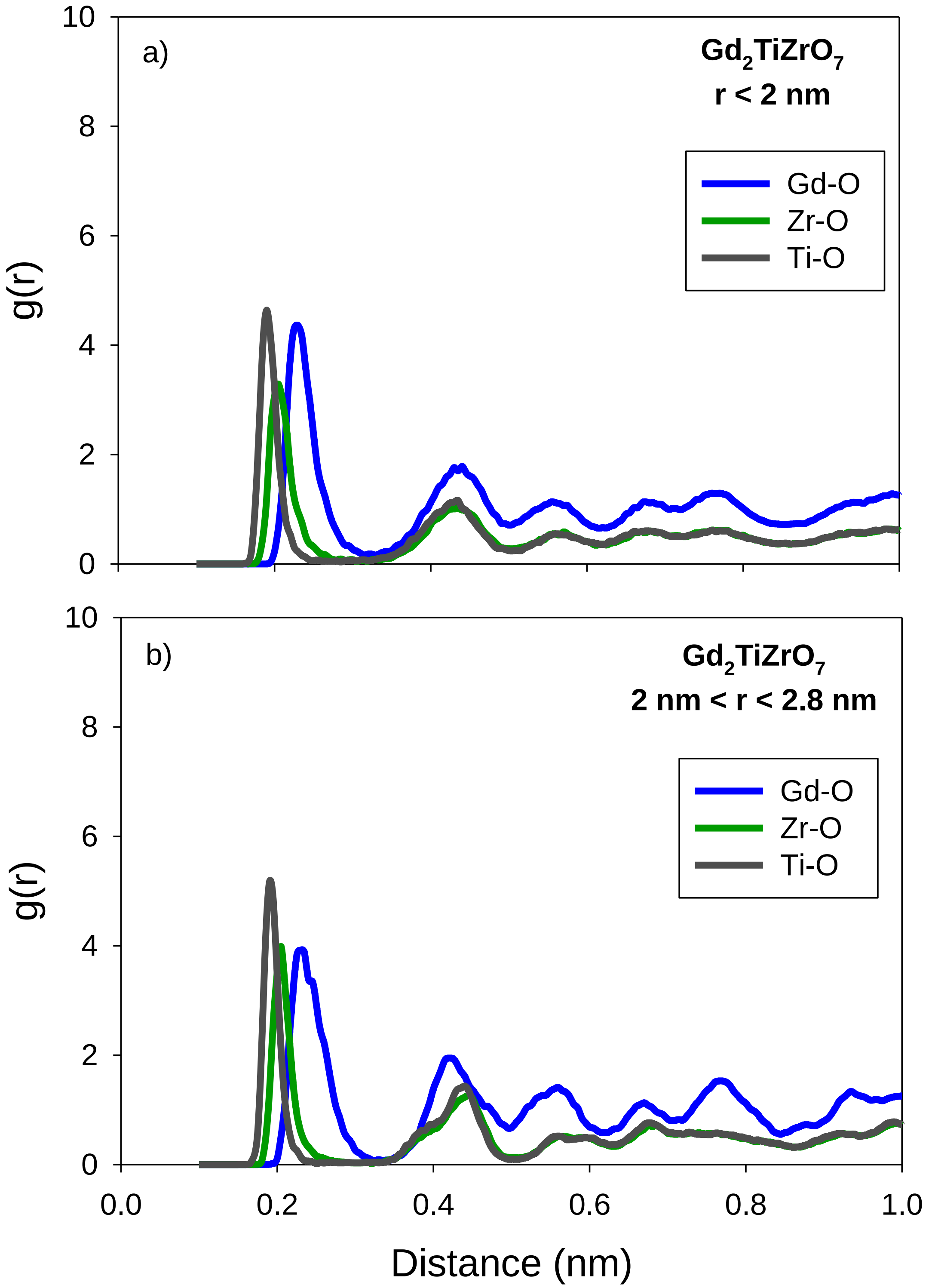


**Fig. S8** Radial distribution functions of Gd-O, Zr-O, and Ti-O pairs in a) the damage core and b) damage periphery in $Gd_2TiZrO_7$ subjected to a thermal spike with energy deposition of 12 keV/nm at 300 K. These regions show peaks characteristic of the fluorite crystal.

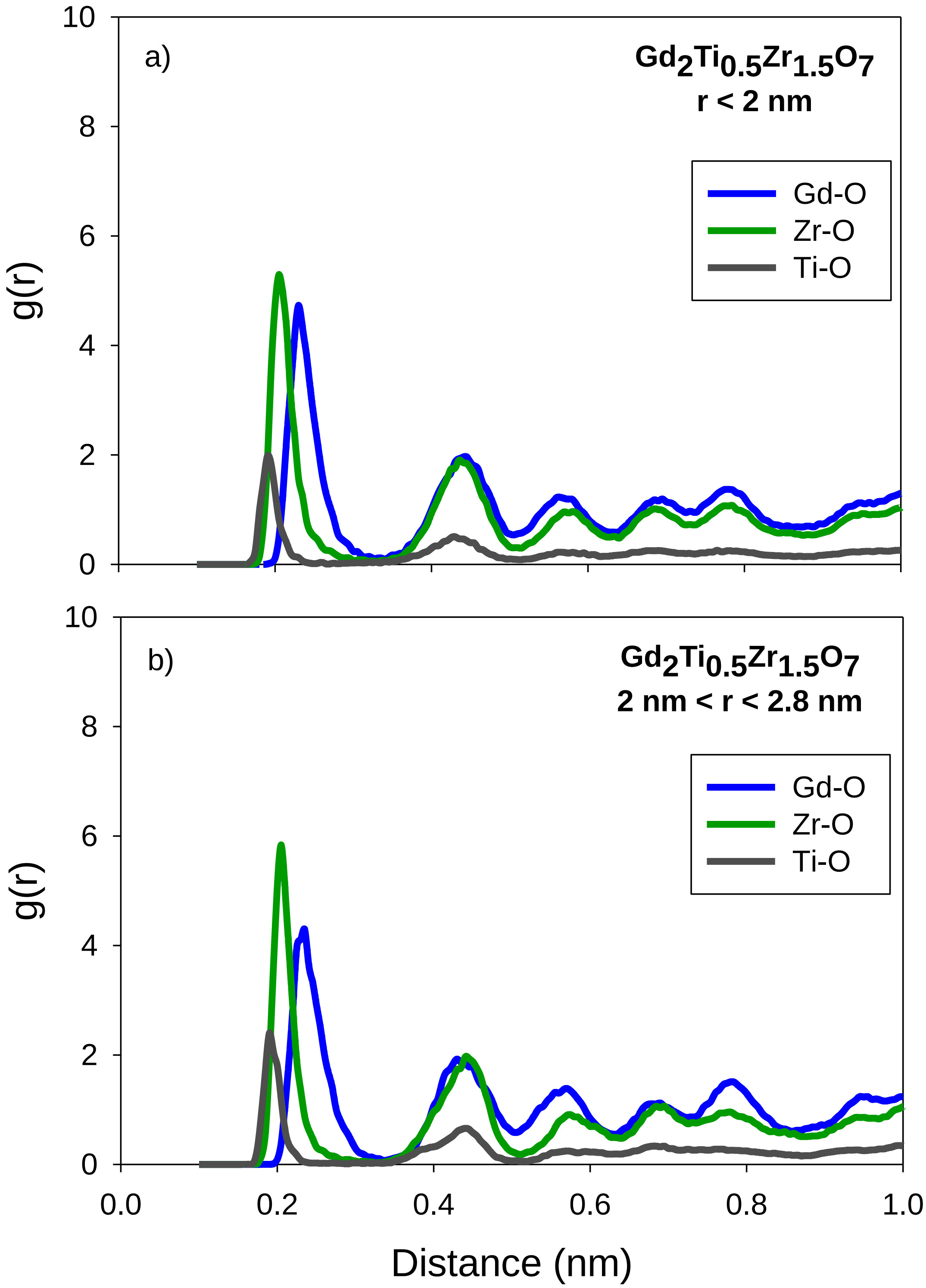


**Fig. S9** Radial distribution functions of Gd-O, Zr-O, and Ti-O pairs in a) the damage core and b) damage periphery in $Gd_2Ti_{0.5}Zr_{1.5}O_7$ subjected to a thermal spike with energy deposition of 12 keV/nm at 300 K. These two regions show peaks characteristic of the fluorite crystal.

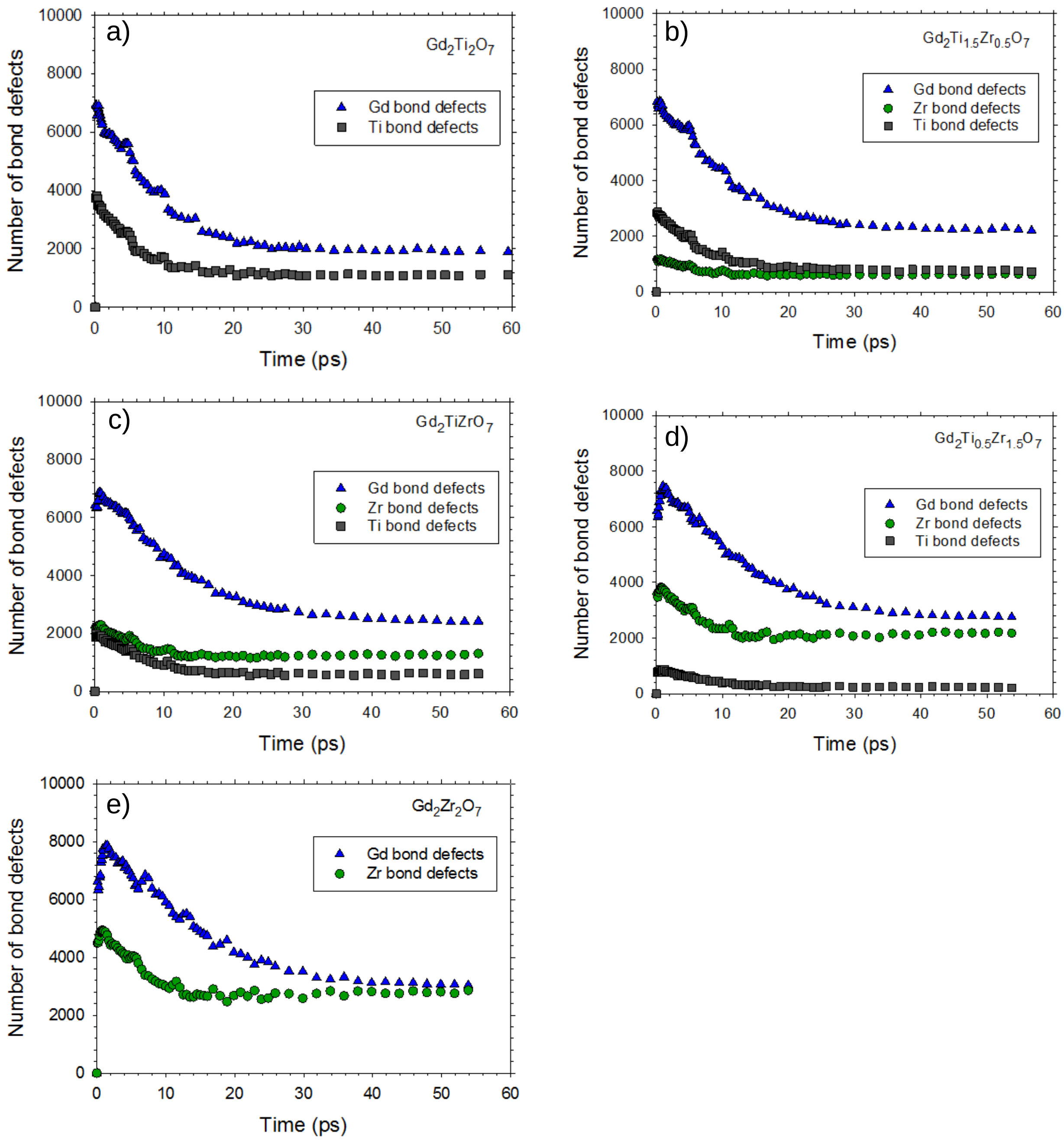


**Fig. S10** Evolution of Gd, Zr and Ti bond defects following a thermal spike with energy deposition of 12 keV/nm at 300 K in a) $Gd_2Ti_2O_7$; b) $Gd_2Ti_{1.5}Zr_{0.5}O_7$; c) $Gd_2TiZrO_7$; d) $Gd_2Ti_{0.5}Zr_{1.5}O_7$; and e) $Gd_2Zr_2O_7$.